2013 IEEE/RSJ International Conference on
Intelligent Robots and Systems (IROS)
November 3-7, 2013. Tokyo, Japan

Hybrid Force/Motion Control and Internal Dynamics of Quadrotors for Tool Operation

Hai-Nguyen Nguyen and Dongjun Lee

Abstract— **This paper presents a hybrid force/motion control framework for quadrotors with a rigid/light tool attached on it. By transforming the quadrotor dynamics into that of the tool-tip position y and applying the passive decomposition to decompose its dynamics into tangential and normal components w.r.t. a contact surface, we design hybrid position/force control. We also elucidate the internal dynamics (i.e., the dynamics hidden from the tool-tip position and yaw angle output and not directly affected by the control action due to the quadrotor's under-actuation), reveal a (seemingly counter-intuitive) necessary condition for internal stability (i.e., tool above the quadrotor, not beneath it), and propose a stabilizing control action to ensure the angular rates still be bounded while preventing the finite-time escape. Simulations are performed to support the theory.**

I. INTRODUCTION

The last decade has witnessed a strong surge of interests in the utilization of quadrotor-type flying robots due to their affordability and simple mechanical structure, the relative easiness to control their center-of-mass position, and the (exciting) promise to expand the current capability of ground-bound robotic systems into the 3-dimensional space including operations in the air. Many strong control techniques have been proposed for the motion control of (the center-of-mass of) the quadrotors: trajectory tracking control [1], [2], [3], teleoperation [4], [5], distributed control [6], [7], to name just few.

These motion control results, however, are mainly for "passive" tasks (i.e., without mechanical interaction with external environments/objects: e.g., surveillance, aerial photography, visual inspection, etc). In contrast, to be truly useful and versatile robotic platforms, the quadrotors should be able to perform "active" tasks, involving mechanical interactions with external environments/objects/humans (e.g., grasping [8], manipulation [9], contact operation [10], etc.). Unfortunately, the control results to enable quadrotors to perform such "active" task are much rarer as compared to the plethora of those for their (pure) motion control.

In this paper, we consider the hybrid force/motion control problem [11] for the quadrotors with a rigid tool attached on it, i.e., regulating the tool-tip contact force while driving the tool-tip position on the contact surface. See Fig. 1. Note that, differently from the typical center-of-mass motion control, this hybrid control problem with the tool requires *simultaneous* orientation and translation control of the quadrotor, which is challenging since, for the quadrotor, its translation control (via the thrust input) is coupled with its rotational motion due to its under-actuation property.

More precisely, built upon our recent result in [12], we first transform the quadrotor's full dynamics into that of the tool-tip position y in the Cartesian space. We then apply the passive decomposition [13], [14] to decompose this tool-tip y-dynamics along the tangential and normal directions w.r.t. the contact surface; and, by controlling the former, achieve the motion control on the contact surface, whereas, by controlling the latter, control either the approaching motion to or the contact force against the surface. The desired control actions, designed for these tangential and normal directions, are then mapped to the angular acceleration and the thrust force, with the former realized by the angular torque of the quadrotor.

Nevertheless, with the tool-tip position control, generally arises the problem of internal dynamics [15]. This is because, by controlling the tool-tip position y (and yaw angle), the pitch and roll motions become "hidden" from the control formulation, thereby, constitute internal state[1]. In this paper, we elucidate this internal dynamics for the general quadrotor tool operations; reveal a (seemingly counter-intuitive) necessary condition for the internal stability, i.e., the tool should be above the quadrotor, not beneath it; show that this internal dynamics can even trigger finite-time escape if not properly treated; and propose a preliminary control action to stabilize this internal dynamics (in the sense of bounded velocity) while preventing the finite-time escape.

The hybrid force/motion control of quadrotor, albeit defining one of the most basic tool operations, likely because of the theoretical challenges as stated above, still lacks thorough understanding of its mechanics and proper control frameworks for that. Some related works are as follows. In [16], an extra horizontal propeller is installed on a quadrotor for a vertical climbing task with the quadrotor staying horizontal and maintaining horizontal contact. The hybrid control problem same as ours (with a tool) was considered in [17], where the quadrotor is considered as a *quasi-static* wrench generator, thus, dynamics effect (e.g., Coriolis effect), which turn out to be important for the operation stability as shown in this paper, was not taken into account there. Another relevant results are [18], [19], with

The authors are with the School of Mechanical & Aerospace Engineering and IAMD, Seoul National University, Seoul, Republic of Korea, 151-744. Email: {hainguyen,djlee}@snu.ac.kr

Research supported in part by the Basic Science Research Program of the National Research Foundation (NRF) by the Korea Government (MEST) (2012-R1A2A2A0-1015797).

[1]Or, equivalently, from the 12-dimensional state of the quadrotors, with $y \in \Re^3$ and yaw angle as the output, each with relative degree 2, we still have 4-dimensional internal dynamics.

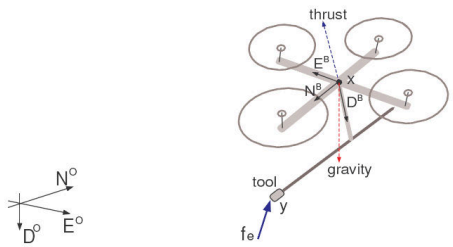

Fig. 1. Quadrotor with a tool

the former and the latter respectively considering only the pitch stability during payload grasping tasks in the sagittal plane and the stability during a (passive) interaction with the environment, thus, not directly applicable to the quadrotor tool-tip hybrid position/force (active) control in E(3) as considered in this paper. Our current paper also significantly extends the results of [12], where only the trajectory tracking and simple tool rotation control (i.e., screw-driver, vertical-jack) are considered with no force control, and the internal dynamics is analyzed only for those simple tool rotation motions.

The rest of this paper is composed as follows. The quadrotor system modeling with a rigid/light tool attached on it is given in Sec. II. The hybrid force/motion control, derived by using the passive decomposition [13], is then presented in Sec. III. The issue of internal dynamics, its stability property and a preliminary stabilizing control design are presented in Sec. IV along with some relevant simulation results. Finally, conclusion is given in Sec. V.

II. SYSTEM MODELING

Consider a quadrotor with the following dynamics [3]

$$m\ddot{x} = -\lambda R e_3 + mge_3 + f_e \tag{1}$$

$$J\dot{\omega} + \omega \times J\omega = \tau + \tau_c, \dot{R} = RS(\omega) \tag{2}$$

where $x \in \Re^3$ is the quadrotor's center-of-mass position represented in the inertial frame $\{O\} := \{N^o, E^o, D^o\}$, $m > 0$ is the mass, $\lambda \in \Re$ is thrust, $R \in SO(3)$ represents the rotation of the body-frame $\{B\} := \{N^B, E^B, D^B\}$ w.r.t the inertial-frame $\{O\}$, $f_e \in \Re^3$ is the tool force represented in $\{O\}$, g is the gravitation constant, and $e_3 = [0, 0, 1]^T$ is the basis vector specifying the down direction. Also, $J \in \Re^3$ is the body-frame rotational inertia, $\omega_i := [\omega_1, \omega_2, \omega_3]^T \in \Re^3$ is the angular velocity of $\{B\}$ relative to $\{O\}$ represented in $\{B\}$, $\tau, \tau_c \in \Re^3$ are the torque input for the quadrotor and the external torque acting at the center-of-mass (defined below) all represented in $\{B\}$ frame, and

$$S(\omega) = \begin{bmatrix} 0 & -\omega_3 & \omega_2 \\ \omega_3 & 0 & -\omega_1 \\ -\omega_2 & \omega_1 & 0 \end{bmatrix} \quad \text{s.t} \quad S(\omega)\nu = \omega \times \nu$$

for any $\nu \in \Re^3$.

Now, suppose that a tool is rigidly-attached to the quadrotor as shown in Fig. 1, whose tip y is located from the center-of-mass as specified by $d = [d_1, d_2, d_3]^T \in \Re^3$ expressed in the body-frame $\{B\}$. Here, we assume $d_2 = 0$ (i.e., tool tip on the N-D plane). Then, the tool tip position (or output) y in the inertial frame $\{O\}$ can be written as

$$y = x + Rd.$$

Also, assume that the tool tip y interacts with the environment through the Cartesian force f_e and the moment τ_e. Then, the disturbance torque τ_c in (2) is given by

$$\tau_c = d \times R^T f_e + R^T \tau_e.$$

In this paper, for the tool operation, we would like to drive the tool tip position y while also regulating the interaction force f_e.

For the tool-tip position y, we can easily show the followings:

$$\dot{y} = \dot{x} + \dot{R}d = \dot{x} + RS(\omega)d \tag{3}$$

$$\ddot{y} = \ddot{x} + R[S(\dot{\omega}) + S^2(\omega)]d \tag{4}$$

Substituting (4) into (1), we can then obtain the following dynamics of the tool tip position y [12]:

$$m\ddot{y} - mR[S(\dot{\omega}) + S^2(\omega)]d = -\lambda R e_3 + mge_3 + f_e \tag{5}$$

which can be rewritten as

$$m\ddot{y} = u + f_e \tag{6}$$

where the *control generation equation* is given by

$$u = mR[S(\dot{\omega}) + S^2(\omega)]d - \lambda R e_3 + mge_3 \tag{7}$$

for which $mR[S(\dot{\omega}) + S^2(\omega)]d$ is the force generated by the rotation of quadrotor represented in end-effector coordinate. In (7), we can consider the thrust λ and the angular acceleration $\dot{w}$ as the control inputs [12]. In the next Sec. III, we will design these controls $\lambda, \dot{w}$ to attain the objective of hybrid position/force control through the tool-tip y of the quadrotor. The peculiar issue of internal dynamics, associated to this hybrid position/force control, is then analyzed in Sec. IV, with some (seemingly counter-intuitive) structural condition for internal stability.

III. HYBRID TOOL FORCE/POSITION CONTROL OF QUADROTOR

A. Passive Decomposition

The basic idea of the hybrid motion/force control [11] is to decompose the system dynamics along the surface (i.e., motion control) and normal to that surface (i.e., force control), while assuming that the contact with the surface is somehow maintained all the time. For the quadrotor tool operation, however, this assumption of contact be maintained all the time is too strict (e.g., approaching to the surface) and also should be satisfied rather than assumed a prior. For this, here, we utilize *passive decomposition* [13], [14], with which we can decompose the tool tip dynamics (5) into the locked system, representing the system's motion tangential to the contact surface; and the shape system, specifying the system's motion normal to the contact surface. Then, by controlling the shape system, we can control the contact

force, while driving the locked system, can achieve a desire motion on the surface, even if the contact assumption is not satisfied at the beginning, as in Fig. 2.

For this, suppose that the working surface can be represented by a set of holonomic constraints of the tool-tip position y s.t.,

$$h(y) = 0$$

where $h(y) \in \Re$ (i.e., 2-dimensional surface embedded in 3-dimensional Cartesian space of $y \in \Re^3$). We assume this h be smooth with full-rank Jacobian (i.e., submersion [13]). Then, we have

$$\frac{\partial h}{\partial y}\dot{y} = 0 \tag{8}$$

which shows that if $\dot{y} \in \text{null}(\partial h/\partial y)$ with $h(y(0)) = 0$, the tool-tip position y will stay on the surface.

Following [13], [14], at each y, the tangent space (velocity space $T_q\mathcal{M}$) and the cotangent space (i.e., force space $T_q^*\mathcal{M}$) of the tool-tip dynamics (5) can split, respectively, s.t

$$T_q\mathcal{M} = \Delta_\top \oplus \Delta_\perp \quad \text{and} \quad T_q^*\mathcal{M} = \Omega_\top \oplus \Omega_\perp$$

where $\Delta_\top \in \Re^{3\times 2}$ identifies the kernel space of $\partial h/\partial y$ (with $\Delta_\top^T\Delta_\top = I$), $\Delta_\perp \in \Re^{3\times 1}$ identifies the orthogonal complement of $\Delta_\top$ w.r.t. the inertia metric m of (5), $\Omega_\top \in \Re^{3\times 2}$ and $\Omega_\perp \in \Re^{3\times 1}$ identify the annihilating co-distributions of $\Delta_\perp$ and $\Delta_\top$ respectively, and $\oplus$ is the direct sum.

With these decomposition of the tangent and co-tangent spaces, we can write the velocity $\dot{y}$ and force of (5) s.t.,

$$\dot{y} = \Delta v = \begin{bmatrix}\Delta_\top & \Delta_\perp\end{bmatrix}\begin{pmatrix} v_l \\ v_h \end{pmatrix} \tag{9}$$

and also

$$u + f_e = \begin{bmatrix}\Omega_\top^T & \Omega_\perp^T\end{bmatrix}\begin{pmatrix} u_l + f_l \\ u_h + f_h \end{pmatrix} \tag{10}$$

for which, since the metric of (5) is Euclidean, following [14], we can obtain the following closed-form matrix expressions: with $\Delta_\top \approx \text{null}(\partial h/\partial y)$, $\Omega_\perp = \partial h/\partial y$, $\Delta_\perp = \Omega_\perp^T(\Omega_\perp\Omega_\perp^T)^{-1}$, and $\Omega_\top = (\Delta_\top^T\Delta_\top)^{-1}\Delta_\top^T$. We can then easily show that

$$\Delta_\top^T\Delta_\perp = 0, \quad \Omega\Delta = I, \quad \frac{dh}{dt} = \Omega_\perp\dot{y} = \Omega_\perp\Delta_\perp v_h = v_h$$

where the last equation clearly shows that v_h is the velocity in the normal direction to the contact surface, while v_l is the velocity component of the tool-tip dynamics (5) tangential to the surface.

Differentiating (9), we can then obtain

$$\ddot{y} = \Delta\dot{v} + \dot{\Delta}v.$$

Inserting this into (6) while left-multiplication by Δ^T yields

$$m\dot{v}_l + Q_l(y,\dot{y})v_l + Q_{lh}(y,\dot{y})v_h = u_l + f_l \tag{11}$$
$$m\dot{v}_h + Q_h(y,\dot{y})v_h + Q_{hl}(y,\dot{y})v_l = u_h + f_h \tag{12}$$

where we call (11) *locked system* (i.e., dynamics along the tangential directions), while (12) *shape system* (i.e., dynamics along the normal direction), both of which inherit the Lagrangian structure and passivity from the original dynamics (6). From the property of the passive decomposition, we also have: Q_l skew-symmetric, $Q_h = 0$ and $Q_{lh}^T = -Q_{hl}$. Refer to [13], [14] for more details on the passive decomposition.

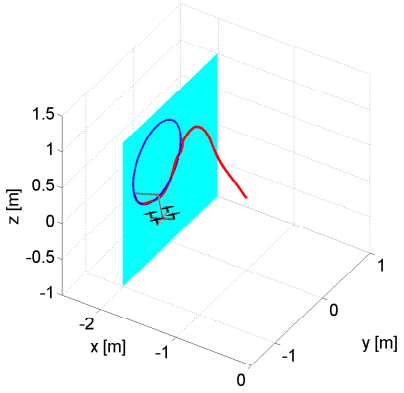

Fig. 2. Hybrid force/position control of quadrotor with a tool attached at $d = [0.35; 0; -0.3]$ under the stabilizing ν_3-action (26).

B. Tangential Motion Control

To drive the tool-tip position y along a certain desired trajectory on the surface, here, we design a trajectory tracking control for the locked system (11). For this, define first $q_l := q_l(y) \in \Re^2$ to be the local coordinate of the surface, with the desired trajectory on the surface given by $q_d(t)$. Differentiating this q_l, we then have

$$\dot{q}_l := \frac{\partial q_l}{\partial y}\dot{y} = \frac{\partial q_l}{\partial y}\Delta_\top v_l$$

where $B = (\frac{\partial q_l}{\partial y}\Delta_\top)^{-1} \in \Re^{2\times 2}$ exists at least locally. With this B, we can further obtain:

$$v_l = B\dot{q}_l, \quad \dot{v}_l = B\ddot{q}_l + \dot{B}\dot{q}_l$$

and, substituting these to (11) and left multiplying by B^{-1}, we have

$$m\ddot{q}_l + B^{-1}(m\dot{B} + Q_lB)\dot{q}_l + B^{-1}Q_{lh}v_h = B^{-1}(u_l + f_l)$$

where we can show that $B^{-1}(m\dot{B} + Q_lB)$ is skew-symmetric. We then design the trajectory tracking control u_l s.t.,

$$\begin{aligned} B^{-1}u_l := {} & B^{-1}Q_{lh}v_h + B^{-1}(m\dot{B} + Q_lB)\dot{q}_l + \\ & m\ddot{q}_d - b(\dot{q}_l - \dot{q}_d) - k(q_l - q_d) - B^{-1}f_l \end{aligned} \tag{13}$$

with which the closed-loop locked system dynamics becomes:

$$m(\ddot{q}_l - \ddot{q}_d) + b(\dot{q}_l - \dot{q}_d) + k(q_l - q_d) = 0$$

implying the stable trajectory tracking on the contact surface.

C. Normal Force Control

For the normal force regulation or approaching motion to the contact surface, here, we design a control for the shape system (12). First, for the free-space motion (i.e., before or

after contact phase), we design the motion control for the shape system (12) s.t.,

$$u_h := Q_{lh} v_l - k_v v_h - k_p (h - h^\star) \tag{14}$$

where $v_h = \dot{h}$ and $h^\star$ is a point close (or slightly within) the contact surface, and $k_v, k_p > 0$ are some suitably-tuned control gains.

On the other hand, if the contact is detected (by using some force sensing), we switch the shape system control from the approaching motion control (14) to the force regulation control:

$$u_h := Q_{lh} v_l - f_d + k_i \int_0^t (f_h - f_d) d\tau - b v_h \tag{15}$$

where $f^d \in \Re$ is the desired contact force, $k_i, b > 0$ are control gains, $Q_{lh} v_l$ is the cancellation of the coupling term to ensure the force regulation regardless of the tangential motion, and the last term $b v_h$ is to enhance stability of this force regulation loop, which can be omitted if the force control starts with small-enough normal velocity v_h. Then, the closed-loop shape system dynamics is given by

$$m \dot{v}_h = f_h - f_d + k_i \int_0^t (f_h - f_d) d\tau - b v_h$$

implying that the force regulation (i.e., $f \to f_d$) with $v_h = \dot{h} \to 0$. With some more assumptions, we may theoretically enforce stability of this controller switching (e.g., [20]).

D. Control Decoding

Once we design the hybrid force/motion controllers for the locked and shape systems (13), (14) and (15), they can be converted into the control action u for the y-dynamics (6) s.t.,

$$u_d = \begin{bmatrix} \Omega_\top^T & \Omega_\perp^T \end{bmatrix} \begin{pmatrix} u_l \\ u_h \end{pmatrix} \tag{16}$$

through (10). Here, recall from (7) that the real control is $(\lambda, \dot{w})$. Thus, to decode this desired control action u_d into $(\lambda, \dot{w})$, we define the desired angular acceleration $\dot{\omega}^d = [\dot{\omega}_1^d, \dot{\omega}_2^d, \dot{\omega}_3^d]^T \in \Re^3$ and the thrust control λ following (7) s.t.,

$$S(d)\dot{\omega}_d + S(\omega)S(d)\omega + \frac{\lambda}{m} e_3 - g R^T e_3 = -\hat{u}_d \tag{17}$$

which can in fact generate any desired control $\hat{u}_d := R^T u_d / m \in \Re^3$ by $(\dot{w}_1, \dot{w}_2, \lambda)$ if and only if $d_3 \neq 0$ (i.e., tool-tip above or below the center-of-mass [12]). Also, note that $||\hat{u}_d|| = ||u_d/m||$.

To drive $\dot{w} \to \dot{w}_d$, we then design the attitude control torque τ for (2) s.t.,

$$\tau = \omega \times J\omega + J \left(\dot{\omega} - \beta \left[\omega - \int_0^t \dot{\omega}^d(s) ds \right] \right) - \tau_c \tag{18}$$

where $\beta > 0$ is the control gain. The closed-loop attitude dynamics is then reduced to

$$\dot{e}_\omega + \beta e_\omega = 0$$

where $e_\omega := \omega(t) - \int_0^t \dot{\omega}^d(s) ds$, implying that $\dot{\omega} \to \dot{\omega}^d$.

This however may result in the instability of internal dynamics. since (17) defines dynamics equation between $\dot{w}$, w and the rotation R as well. As shown in [12] and below, this internal dynamics can be unstable and also result in finite-time escape escape if not treated properly. This issue of internal dynamics was addressed in [12], yet, only limited to some specific motions (i.e., rotation around roll or pitch axes). In this work, we generalize the result of [12] to a general motion of the tool-tip dynamics (5) of the quadrotor, which in fact is applicable not only to the hybrid force/motion control but also other control objects as well (e.g.., trajectory tracking [12]).

IV. INTERNAL DYNAMICS OF QUADROTOR DURING TOOL OPERATION

A. Internal Dynamics and Equilibrium

As mentioned above, the control decoding (17) defines an internal dynamics between $\dot{w}, w$ and R. In this Sec. IV, we reveal this internal dynamics of quadrotors during the tool operation and analyze its stability property. Based upon this, we also suggest a (seemingly counter-intuitive) structural condition for the necessity of this internal dynamics local stability and also propose a preliminary control action to globally stabilize this internal dynamics (in the sense of bounded w).

For this, notice first that the decoding equation (17) defines only two-dimensional internal dynamics, since $S(d)$ is singular with $\text{rank}(S(d)) = 2$. We may then decompose w s.t.,

$$\omega = [\Sigma_\top \quad \Sigma_\perp] \nu = \Sigma \nu \tag{19}$$

with

$$\Sigma := \frac{1}{\alpha} \begin{bmatrix} -d_3 & 0 & d_1 \\ 0 & \alpha & 0 \\ d_1 & 0 & d_3 \end{bmatrix}$$

where $\alpha = \sqrt{d_1^2 + d_3^2}$ and $\Sigma = \Sigma^{-1}$. Here, note that the last column of Σ characterizes the nullspace of $S(d)$, while the first two the row space of $S(d)$, the components of w in each of these spaces respectively given by ν_3 and ν_1, ν_2, with $\nu := [\nu_1; \nu_2; \nu_3] \in \Re^3$.

Using this new variable ν, we can then rewrite (17) s.t.,

$$\begin{bmatrix} -d_3 \dot{\nu}_2 \\ -\alpha \dot{\nu}_1 \\ d_1 \dot{\nu}_2 \end{bmatrix} + \begin{bmatrix} d_1 \nu_1^2 + d_1 \nu_2^2 + d_3 \nu_1 \nu_3 \\ -\alpha \nu_2 \nu_3 \\ d_3 \nu_1^2 + d_3 \nu_2^2 - d_1 \nu_1 \nu_3 \end{bmatrix} + \begin{bmatrix} 0 \\ 0 \\ \frac{\lambda}{m} \end{bmatrix} - g R^T e_3 = -\hat{u}_d \tag{20}$$

which defines the internal dynamics of $\dot{\nu}_1$ and $\dot{\nu}_2$, as the last line contains the control input λ and the dynamics of $\dot{\nu}_3$ vanishes when combined with $S(d)$ in (17).

Our notion of internal dynamics should also capture the evolution of the quadrotor's rotation angles. This, however, is rather difficult to directly see from (20), as this rotation motion is given by the rotation matrix $R \in$ SO(3). To make the internal dynamics easier to see, here, we write the internal

dynamics using the roll, pitch and yaw parameterization. Then, we have the following relation:

$$\frac{d}{dt}[\phi,\theta,\psi]^T = \Gamma\omega = \Gamma\Sigma\nu \tag{21}$$

where ϕ,θ,ψ are the yaw, pitch and roll angles, with $|\theta| < \pi/2$, and

$$\Gamma(\theta,\psi) := \begin{bmatrix} 0 & \frac{\sin\psi}{\cos\theta} & \frac{\cos\psi}{\cos\theta} \\ 0 & \cos\psi & -\sin\psi \\ 1 & \frac{\sin\theta\sin\psi}{\cos\theta} & \frac{\sin\theta\cos\psi}{\cos\theta} \end{bmatrix}$$

Then, from (20), the total internal dynamic of the quadrotor during the tool operation control is given by

$$\frac{d}{dt}\big(\theta,\psi,\nu_1,\nu_2\big)^T = \mathcal{F}(\theta,\psi,\nu_1,\nu_2) + \big(0,0,\tfrac{1}{\alpha}\hat{u}_{d2},\tfrac{1}{d_3}\hat{u}_{d1}\big)^T \tag{22}$$

where each component of $\mathcal{F} \in \Re^4$ is given by

$$\begin{aligned}
\mathcal{F}_1 &= -\tfrac{d_1}{\alpha}\nu_1\,\mathrm{s}\,\psi + \nu_2\,\mathrm{c}\,\psi - \tfrac{d_3}{\alpha}\nu_3\,\mathrm{s}\,\psi \\
\mathcal{F}_2 &= -\tfrac{d_3}{\alpha}\nu_1 + \tfrac{d_1}{\alpha}\nu_1\,\mathrm{t}\,\theta\,\mathrm{c}\,\psi + \nu_2\,\mathrm{t}\,\theta\,\mathrm{s}\,\psi + \tfrac{d_1}{\alpha}\nu_3 + \tfrac{d_3}{\alpha}\,\mathrm{t}\,\theta\,\mathrm{c}\,\psi\nu_1\nu_3 \\
\mathcal{F}_3 &= -\nu_2\nu_3 - \tfrac{g}{\alpha}\,\mathrm{c}\,\theta\,\mathrm{s}\,\psi \\
\mathcal{F}_4 &= -\gamma(\nu_1^2+\nu_2^2) + \nu_1\nu_3 + \tfrac{g}{d_3}\,\mathrm{s}\,\theta
\end{aligned}$$

where $\mathrm{s}\star = \sin\star, \mathrm{c}\star = \cos\star, \mathrm{t}\star = \tan\star$, and $\gamma := -d_1/d_3$. Here, the dynamics of yaw angle ϕ does not constitute a part of the internal dynamics, since the expression of $\dot{\phi}$ contains ν_3, which can be assigned arbitrary, thus, considered as a control input. This fact can also seen by that, if we choose the system's output to be $(y,\phi) \in \Re^4$, the relative degree of each variable is two, thus, we only have 4-dimensional internal dynamics as specified in (22). This then means that (22) constitutes the full internal dynamics of the quadrotor, when its tool-tip position y and the yaw angle ϕ are controlled according to certain control objectives.

The internal dynamics (22), with $u_d = 0$, possesses two equilibria: $[\theta,\psi,\nu_1,\nu_2] = [0,0,0,0]$ and $[\theta,\psi,\nu_1,\nu_2] = [0,\pi,0,0]$, the former representing the case of quadrotor's center-of-mass located below (or above, resp.) the tool-tip if $d_3 < 0$ (or $d_3 > 0$, resp.); while the latter the case of quadrotor's center-of-mass located above (or below, resp.) the tool-tip if $d_3 < 0$ (or $d_3 > 0$, resp.).

To see the local stability of each equilibrium, we now perform the linearization of $\mathcal{F}(\theta,\psi,\nu_1,\nu_2)$. For the equilibrium $[\theta,\psi,\nu_1,\nu_2] = [0,0,0,0]$, we can obtain:

$$\begin{bmatrix}\dot{\theta}\\ \dot{\psi}\\ \dot{\nu}_1\\ \dot{\nu}_2\end{bmatrix} = \begin{bmatrix} 0 & 0 & 0 & 1 \\ 0 & 0 & -\frac{d_3}{\alpha} & 0 \\ 0 & -\frac{g}{\alpha} & 0 & 0 \\ \frac{g}{d_3} & 0 & 0 & 0 \end{bmatrix}\begin{bmatrix}\theta\\ \psi\\ \nu_1\\ \nu_2\end{bmatrix} \tag{23}$$

with the characteristic polynomial given by

$$\lambda^4 + \frac{g(-\alpha^2 - d_3^2)}{d_3\alpha^2}\lambda^2 + \frac{gd_3}{d_3\alpha^2} = 0.$$

We then have

$$\lambda_1^2 = \frac{g}{d_3}, \quad \lambda_2^2 = \frac{gd_3}{\alpha^2}$$

implying that, if $d_3 > 0$, the origin of the internal dynamics (22) is unstable.

On the other hand, for the equilibrium $[\theta,\psi,\nu_1,\nu_2] = [0,\pi,0,0]$, the linearization of (22) with $\hat{u}_d = 0$ is given by

$$\begin{bmatrix}\dot{\theta}\\ \dot{\psi}\\ \dot{\nu}_1\\ \dot{\nu}_2\end{bmatrix} = \begin{bmatrix} 0 & 0 & 0 & -1 \\ 0 & 0 & -\frac{d_3}{\alpha} & 0 \\ 0 & \frac{g}{\alpha} & 0 & 0 \\ \frac{g}{d_3} & 0 & 0 & 0 \end{bmatrix}\begin{bmatrix}\theta\\ \psi\\ \nu_1\\ \nu_2\end{bmatrix} \tag{24}$$

whose poles satisfy

$$\lambda_1^2 = -\frac{g}{d_3}, \quad \lambda_2^2 = -\frac{gd_3}{\alpha^2}$$

implying that the internal dynamics (22) will be unstable in the neighborhood of $[\theta,\psi,\nu_1,\nu_2] = [0,\pi,0,0]$ if $d_3 < 0$.

Note then that the instability case for the two linearized dynamics (23)-(24), that is, $d_3 > 0$ at $(\theta,\psi) = (0,0)$ for (23) and $d_3 < 0$ at $(\theta,\psi) = (0,\pi)$ for (24) in fact represent the same situation, that is, the quadrotor's center-of-mass x is located above the tool-tip position y. On the other hand, this observation says that the configuration of the quadrotor with its center-of-mass x located below the tool-tip position y can be stable, as frequently observed through our simulations, although the above linearization analysis cannot provide a definite answer for its (local) stability. This analysis shows that, for internal dynamics stability for the quadrotor tool-operation, the tool-tip should be attached above the quadrotor, not below it, although the latter would sound more reasonable at a first glance (and also typically aimed for in practice).

This can also be explained as follow. If the tool-tip is below the quadrotor, the center-of-mass of the total system will be located above the tool-tip position (i.e., $d_3 > 0$), thus, if we want to, for example, regulate the tool-tip position, the total system would behave similar to the inverted pendulum (around $\psi = 0$) as can be seen from (23) (i.e., saddle with two unstable and two stable poles). On the other hand, if the tool is attached above the quadrotor (i.e., $d_3 < 0$), the system would behave similar to the (stable) downward pendulum as again can be seen from (23) (i.e., pure imaginary poles). This seemingly counter-intuitive condition for the internal dynamics stability is summarized in the following Th. 1, which extends a similar result in [12] derived only for some specific tool-operation modes (i.e., pure rotation along the N-axis or E-axis with the tool-tip position y fixed) to general quadrotor tool operation.

Theorem 1: Consider the quadrotor performing a tool operation, with the tool-tip located at $d = [d_1, 0, d_3]^T$ as measured in its body NED-frame $\{B\}$ from its center-of-mass x. Then, a necessary condition for the internal dynamics stability at the equilibrium $(\theta,\psi,\nu_1,\nu_2) = 0$ is $d_3 < 0$ (i.e., tool attached above the quadrotor).

B. Stabilizing (ν_1,ν_2) Internal Dynamics

Now, suppose that we set $d_3 < 0$ to satisfy the necessary condition for the stability of the equilibrium $(\theta,\psi,\nu_1,\nu_2) = 0$. Even though the above linearization analysis does not

provide a definite answer for the (local) stability of this equilibrium $(\theta, \psi, \nu_1, \nu_2) = 0$, we could still observe from our simulations that the system behaves at least locally Lyapunov stable around this equilibrium, mimicking the behavior of a downward pendulum. We however also observed that, if the state deviates far from this equilibrium, or if we set d_1 to be much larger than d_3, the quadrotor system could go easily unstable.

This is in fact due to the nonlinear quadratic velocity coupling in the internal dynamics, which is capable to induce finite-time escape [21]. To better see this, let us rewrite the ν_1 and ν_2 internal dynamics in (20) s.t.,

$$\begin{bmatrix}\dot{\nu}_1\\ \dot{\nu}_2\end{bmatrix} = \begin{bmatrix}0\\ -\gamma(\nu_1^2+\nu_2^2)\end{bmatrix} + \begin{bmatrix}-\nu_2\\ \nu_1\end{bmatrix}\nu_3 + \begin{pmatrix}\bar{u}_1\\ \bar{u}_2\end{pmatrix} \tag{25}$$

where $\gamma = -d_1/d_3$, $\bar{u}_1 = -\hat{u}_2/\alpha$ and $\bar{u}_2 = -\hat{u}_1/d_3$, with $\hat{u} = [\hat{u}_1; \hat{u}_2; \hat{u}_3] := R^T(ge_3 - u_d/m)$. Here, if the quadrotor behaves as we would like, u_d would be bounded, and so will be $\bar{u}_1$ and $\bar{u}_2$, which we may then consider as bounded/measurable disturbance for (25). On the other hand, the quadratic term with γ in (25), always pushing the point (ν_1, ν_2) downward on the (ν_1, ν_2) plane, can in fact trigger the finite-time escape when $\nu_2 < 0$, whose tendency gets more intense as $|d_1/d_3|$ gets larger [21].

Now, suppose that we want to suppress the possibility of this finite-time escape, without which we would not be able to achieve stable tool operation by the quadrotors with $d_3 < 0$. For this, we may then consider ν_3 as the control input to (globally) stabilize the internal dynamics of ν_1 and ν_2, which can be indeed arbitrarily assignable (see Sec. IV-A). However, the effectiveness of this control ν_3 for (25) is limited, as its action is only along the tangential direction to the circle on the (ν_1, ν_2) plane with the radius $\sqrt{\nu_1^2+\nu_2^2}$ and with the center at the origin, as shown by the vector multiplying ν_3 in (25).

Notice from (25) that we can directly control ν_1 as long as $\nu_2 \neq 0$. However, the quadratic term with γ in (25) indicates always drives (ν_1, ν_2) downward in the (ν_1, ν_2) plane. This then means that, when $\nu_2 > 0$, the control ν_3 can easily pull the state (ν_1, ν_2) towards the origin, while when $\nu_2 < 0$, all we can do is to drive (ν_1, ν_2) away from the ν_2 axis as fast as possible so that (ν_1, ν_2) can come back to the upper side of the plane (i.e., $\nu_2 > 0$) as quickly as possible. To achieve this property, we propose the following control action for ν_3:

$$\nu_3 = k\nu_1(1+\nu_2^2) \tag{26}$$

where $k = -\epsilon\frac{d_1}{d_3}$, $\epsilon > 0$. It can be seen that, if the disturbance $\bar{u}_i$ is not so large, the control action (26) would maintain the boundedness of (ν_1, ν_2) by driving the state to the upside of (ν_1, ν_2) space, thereby, preventing the issue of finite-time escape. Note that, once this (desired) ν_3-action (26) is adopted, all (w_1^d, w_2^d, w_3^d) are determined via (19), which can then be achieved by applying the control torque (18) to the rotation dynamics (2). Here, notice also from (25) that, even if we cannot control the direction of control action ν_3, we can control its magnitude and direction however we want.

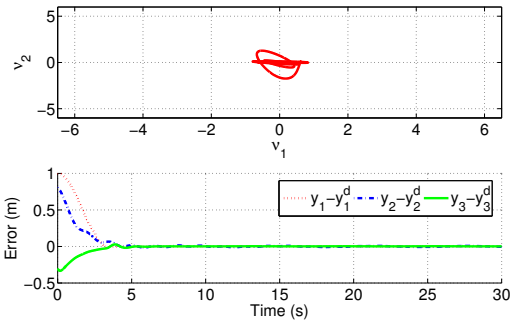

Fig. 3. Hybrid position/force control with $d = [0.15; 0; -0.4]$: stable even without stabilizing control (26).

Note from (26) that, with a small enough disturbance $\bar{u}_i$, the state (ν_1, ν_2) of (25) with the control action (26) would eventually move up to the first and second quadrants and converge to the ν_2-axis in the (ν_1, ν_2) plane since ν_3 is in proportion to ν_2^2. However, along this ν_2-axis (i.e., $\dot{\nu}_1 = \nu_1 = 0$), the control action ν_3 for the ν_2-dynamics (25) vanishes. To analyze system's behavior along this ν_2-axis, let us consider the full internal dynamics (22) again, which, with $\nu_1 = 0$, then reduces to:

$$\dot{\nu}_1 = -\frac{g}{\alpha}\cos\theta\sin\psi, \quad \dot{\nu}_2 = -\gamma\nu_2^2 + \frac{g}{d_3}\sin\theta$$
$$\dot{\theta} = \cos\psi\nu_2, \quad \dot{\psi} = \tan\theta\sin\psi\nu_2.$$

From these equations with $\dot{\nu}_1 = 0$, we can then also obtain $\sin\psi = 0$, implying that $\psi = 0$, as we exclude $\psi = \pi$ (unstable equilibrium) with $d_3 < 0$. We then have $\dot{\theta} = \nu_2$ and the ν_2-dynamics on the ν_2-axis is reduced to

$$\ddot{\theta} = -\gamma\dot{\theta}^2 + \frac{g}{d_3}\sin\theta \tag{27}$$

which is again the dynamics of the (stable) downward pendulum ($d_3 < 0$) with the quadratic perturbation $\gamma\dot{\theta}^2$, that will be locally marginally stable if $d_3 < 0$ [12].

This control action (26) can then allow us to avoid finite-time escape even when d_1 is much longer than d_3 or the the initial value of (ν_1, ν_2) is not so small. Recall from Sec. IV-A that, if (ν_1, ν_2) is small enough or $|\gamma| = |d_1/d_3|$ small enough, even without this control action (26), the quadrotor tool operation would be stable if $d_3 < 0$ (i.e., tool above the quadrotor). See Fig. 3, where the quadrotor tool operation stability can be maintained with $d_3 < 0$ ($d = [0.15; 0; -0.4]$) even without stabilizing control (26).

However, if we increase d_1/d_3 larger, even if $d_3 < 0$, the tool operation can become unstable with possible finite-time escape (e.g., $d = [0.35; 0; -0.3]$: not shown here). This unstable operation with $d_3 < 0$ can then be stabilized by the ν_3-action (26) as shown in Fig. 4, where we can see that, at the moment when the tool contacts with the wall, to produce a (large) counteracting force, the quadrotor tilts, pushing (ν_1, ν_2) into "dangerous area" of the phase-portrait (i.e., forth quadrant: see Fig. 4). The ν_3-action then reacts to drive (ν_1, ν_2) to "safe area" of Fig. 4 (i.e., upside), thereby, stabilize (ν_1, ν_2). Of course, even if d_1/d_3 is small, the tool

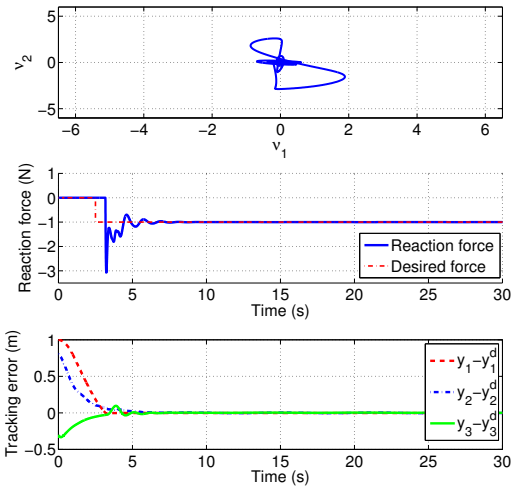

Fig. 4. Hybrid position/force control with $d = [0.35; 0; -0.3]$: stable operation with stabilizing control (26).

operation becomes unstable with finite-time escape, when we set $d_3 > 0$ (e.g., $d = [0.2; 0; 0.35]$: not shown here).

Note that, when deriving this (ν_1, ν_2)-stabilizing action (26), we just consider the effect of gravity embedded in the disturbance $\bar{u}_i$. This then means that the ν_3-action (26) can also stabilize (ν_1, ν_2) even if $d_3 > 0$ (e.g., $d = [0.35; 0; 0.3]$: not shown here), although, in this case, we found the quadrotor converges to the equilibrium $(\theta, \psi) = (0, \pi)$, again attaining the stable posture (i.e., with the tool above the quadrotor).

As can be seen in (22), since the ν_3-action does not consider the rotational motion itself, the quadrotor may collide with the contact surface, even if the stability of the operation is ensured. How to include the information of this rotation motion into the ν_3-action (e.g., changing k depending on the motion of the quadrotor to prevent the collision), along with its full stability analysis, is a topic for future research.

V. CONCLUSION

In this paper, the hybrid force/motion control regarding full nonlinear dynamics and under-actuation of quadrotors with a light/rigid tool attached on it is presented. We first transform the quadrotor dynamics into that of the tool-tip position; and decompose it into the tangential and normal directions w.r.t. the contact surface by using the passive decomposition. We then design hybrid force/motion control by designing controls for each of this tangential and normal dynamics, and convert it into the desired thrust and angular torque inputs. We also elucidate the internal dynamics, which generally arises under a tool-tip position control due to the quadrotor's under-actuation, reveal necessary condition for internal stability (i.e., tool above the quadrotor) and possibility of finite-time escape, and also propose a preliminary stabilizing action to ensure boundedness of velocities while preventing the finite-time escape. Some future research direction includes: 1) full analysis and expansion of the stabilizing ν_3-action (26) for collision-free quadrotor tool operation; and 2) extension of our results to other types of aerial robots.

REFERENCES

[1] R. Mahony and T. Hamel. Robust trajectory tracking for a scale model autonomous helicopter. *Int'l Journal of Robust and Nonlinear Control*, 14(12):1035–1059, 2004.

[2] M-D Hua, T Hamel, P Morin, and C Samson. A control approach for thrust-propelled underactuated vehicles and its application to vtol drones. *IEEE Transactions on Automatic Control*, 54(8):1837–1853, 2009.

[3] D. J. Lee, C. Ha, and Z. Zuo. Backstepping control of quadrotor-type uavs and its application to teleoperation over the internet. In S. Lee, H. Cho, K-J. Yoon, and J. Lee, editors, *Intelligent Autonomous Systems 12*, volume 194 of *Advances in Intelligent Systems & Computing*, pages 217–225. Springer Berlin Heidelberg, 2013.

[4] A. Franchi, C. Secchi, H. I. Son, H. H. Bülthoff, and P. R. Giordano. Bilateral teleoperation of groups of mobile robots with time-varying topology. *IEEE Transactions on Robotics*, 28(5):1019–1033, 2012.

[5] D. J. Lee, A. Franchi, H-I. Son, C. Ha, H. H. Bülthoff, and P. R. Giordano. Semi-autonomous haptic teleoperation control architecture of multiple unmanned aerial vehicles. *IEEE/ASME Transactions on Mechatronics*, 18(4):1334–1345, 2013.

[6] A. Abdessameud and A. Tayebi. Formation control of vtol uavs without linear-velocity measurements. In *Pro. American Control Conference*, pages 2107–2112, 2010.

[7] D. J. Lee. Distributed backstepping control of multiple thrust-propelled vehicles on balanced graph. *Automatica*, 48(11):2971–2977, 2012.

[8] R. Spica, A. Franchi, G. Oriolo, H. H. Bülthoff, and P. R. Giordano. Aerial grasping of a moving target with a quadrotor uav. In *Pro. IEEE/RSJ Int'l Conference on Intelligent Robots and Systems*, pages 4985–4992, 2012.

[9] N. Michael, J. Fink, and V. Kumar. Cooperative manipulation and transportation with aerial robots. *Autonomous Robots*, 30(1):73–86, 2011.

[10] L. Marconi and R. Naldi. Control of aerial robots: Hybrid force and position feedback for a ducted fan. *IEEE Control Systems Magazine*, 32(4):43–65, 2012.

[11] R. M. Murray, Z. Li, and S. S. Sastry. *A mathematical introduction to robotic manipulation*. CRC Press, 1994.

[12] D. J. Lee and C. S. Ha. Mechanics and control of quadrotor for tool operation. In *Pro. ASME Dynamic Systems and Control Conference*, 2012.

[13] D. J. Lee and P. Y. Li. Passive decomposition of multiple mechanical systems under motion coordination requirements. *IEEE Transactions on Automatic Control*, 58(1):230–235, 2013.

[14] D. J. Lee. Passive decomposition and control of nonholonomic mechanical systems. *IEEE Transactions on Robotics*, 26(6):978–992, 2010.

[15] J. J. E. Slotine and W. P. Li. *Applied nonlinear control*. Prentice Hall NJ, 1991.

[16] A. Albers, S. Trautmann, T. Howard, T-A Nguyen, M. Frietsch, and C. Sauter. Semi-autonomous flying robot for physical interaction with environment. In *Pro. IEEE Conference on Robotics Automation and Mechatronics*, pages 441–446, 2010.

[17] S. Bellens, J. De Schutter, and H. Bruyninckx. A hybrid pose/wrench control framework for quadrotor helicopters. In *Pro. IEEE Int'l Conference on Robotics and Automation*, pages 2269–2274, 2012.

[18] P. E. I. Pounds, D. R. Bersak, and A. M. Dollar. Stability of small-scale uav helicopters and quadrotors with added payload mass under pid control. *Autonomous Robots*, 33(1-2):129–142, 2012.

[19] P. E. I. Pounds and A. M. Dollar. Uav rotorcraft in compliant contact: Stability analysis and simulation. In *Pro. IEEE/RSJ Int'l Conference on Intelligent Robots and Systems*, pages 2660–2667, 2011.

[20] T. J. Tarn, Y. Wu, N. Xi, and A. Isidori. Force regulation and contact transition control. *IEEE Control Systems Magazine*, 16(1):32–40, 1996.

[21] R. Sepulchre, M. Jankovic, and P. Kokotovic. *Constructive nonlinear control*. Springer-Verlag London, 1997.